Carbohydrate Polymers 84 (2011) 96–102

Contents lists available at ScienceDirect

Carbohydrate Polymers

journal homepage: www.elsevier.com/locate/carbpol

Structural characterization of bacterial cellulose produced by *Gluconacetobacter swingsii* sp. from Colombian agroindustrial wastes

Cristina Castro[a,1], Robin Zuluaga[b,*], Jean-Luc Putaux[c], Gloria Caro[a], Iñaki Mondragon[d], Piedad Gañán[a]

[a] *School of Engineering, Chemical Engineering Program, New Materials Research Group, Pontificia Bolivariana University, Circular 1 # 70-01, Medellín, Colombia*
[b] *School of Engineering, Agro-Industrial Engineering Program, New Materials Research Group, Pontificia Bolivariana University, Circular 1 # 70-01, Medellín, Colombia*
[c] *Centre de Recherches sur les Macromolécules Végétales (CERMAV-CNRS), BP 53, F-38041 Grenoble cedex 9, France (affiliated with Université Joseph Fourier and member of the Institut de Chimie Moléculaire de Grenoble)*
[d] *"Materials + Technologies" Group, Chemical & Environmental Engineering Department, Polytechnic School, Universidad del País Vasco/Euskal Herriko Unibertsitatea, Pza. Europa, 1, 20018 Donostia – San Sebastián, Spain*

ARTICLE INFO

Article history:
Received 20 September 2010
Received in revised form 23 October 2010
Accepted 27 October 2010
Available online 4 November 2010

Keywords:
Acetobacter xylinum
Bacterial cellulose
Agroindustrial residues
Crystal structure

ABSTRACT

Bacterial cellulose microfibrils from non-conventional sources were produced by *Gluconacetobacter swingsii* sp. Agroindustrial residues such as pineapple peel juice and sugar cane juice were used as culture media. Hestrin and Schramm's medium was used as a reference. The production of bacterial cellulose from pineapple peel juice (2.8 g/L) was higher than that produced from Hestrin and Schramm's medium (2.1 g/L). The carbon and nitrogen resources in pineapple peel and sugar cane juice were sufficient for the microorganism development. Ribbon-like microfibrils with a width of 20–70 nm were observed in all media. Changes in crystallinity and mass fraction of the I_α allomorph were observed. The aggregation of cellulose chains into microfibrils was slightly hindered by other polysaccharides in the agroindustrial waste that adhered to the surface of the subfibrils. In conclusion, agroindustrial residues can be used as a culture medium to produce bacterial cellulose with low cost for large-scale industrial production.

1. Introduction

Cellulose, the most abundant biopolymer in Nature, can be synthesized by plants, some animals and a large number of microorganisms, as is the case with *Gluconacetobacter* (formerly *Acetobacter*) (Brown, 1886a,b). This is a gram-negative bacterium, strictly aerobic, capable of producing cellulose extracellularly at temperatures between 25 and 30 °C and pH from 3 to 7 (Bielecki, Krystynowicz, Turkiewicz, & Kalinowska, 2005; Iguchi, Yamanaka, & Budhiono, 2000), using glucose, fructose, sucrose, mannitol, among others, as carbon sources (Ramanaka, Tomar, & Singh, 2000; Heo & Son, 2002). The bacteria synthesize cellulose as a primary metabolite. This synthesis mechanism helps the aerobic bacteria to move to the oxygen-rich surface. Moreover, the cellulose pellicle is produced to protect the cells from ultraviolet light and retain moisture (Klemm, Shumann, Udhardt, & Marsch, 2001).

Bacterial cellulose is synthesized in three stages. In the first stage, glucose molecules are polymerized (formation of β-1,4-glucosidic linkages) between the outer and cytoplasm membranes, forming cellulose changes. 10–15 parallel chains form a 1.5 nm-wide protofibril. In a second step, several protofibrils are assembled into 2–4 nm wide microfibrils, and, in a third step a bundle of microfibrils are assembled into a 20–100 nm-wide ribbon. A matrix of interwoven ribbons constitutes the bacterial cellulose pellicle (Iguchi et al., 2000; Klemm et al., 2001). The formation of the pellicle can be modified by strong aeration during agitated cultures or by the presence of certain substances that can affect the supramolecular organization of microfibrils by disrupting the formation of hydrogen bonds between cellulose chains (Bootten, Harris, Melton, & Newman, 2008; Hirai, Tsuji, Yamamoto, & Horii, 1998; Tokoh, Takabe, Fujita, & Saiki, 1998; Tokoh, Takabe, Sujiyama, & Fujita, 2002; Watanabe, Tabuchi, Moringa, & Yoshinaga, 1998; Whitney, Brigham, Darke, Reid, & Gidley, 1998; Yamamoto & Horii, 1994, 1996).

In terms of chemical structure, bacterial cellulose is identical to that produced by plants. However, it exhibits higher crystallinity, water-holding capacity, mechanical strength and purity. It contains no lignin, hemicellulose or other natural components. These features make it an interesting raw material for applications as nutritional component (Bielecki et al., 2005), artificial skin (Fontana et al., 1990), composite reinforcement, electronic paper (Jonas & Farah, 1998), flexible display screens (Nakagaito, Nogi, & Yano, 2010) and in traditional applications where plant cellulose is used. However, due to the high cost of carbon sources for

* Corresponding author. Tel.: +57 4 3544532; fax: +57 4 3544532.
E-mail addresses: cristina.castro@upb.edu.co (C. Castro), robin.zuluaga@upb.edu.co (R. Zuluaga).
[1] Tel.: +57 4 3544532; fax: +57 4 35445432.

0144-8617/$ – see front matter © 2010 Elsevier Ltd. All rights reserved.
doi:10.1016/j.carbpol.2010.10.072

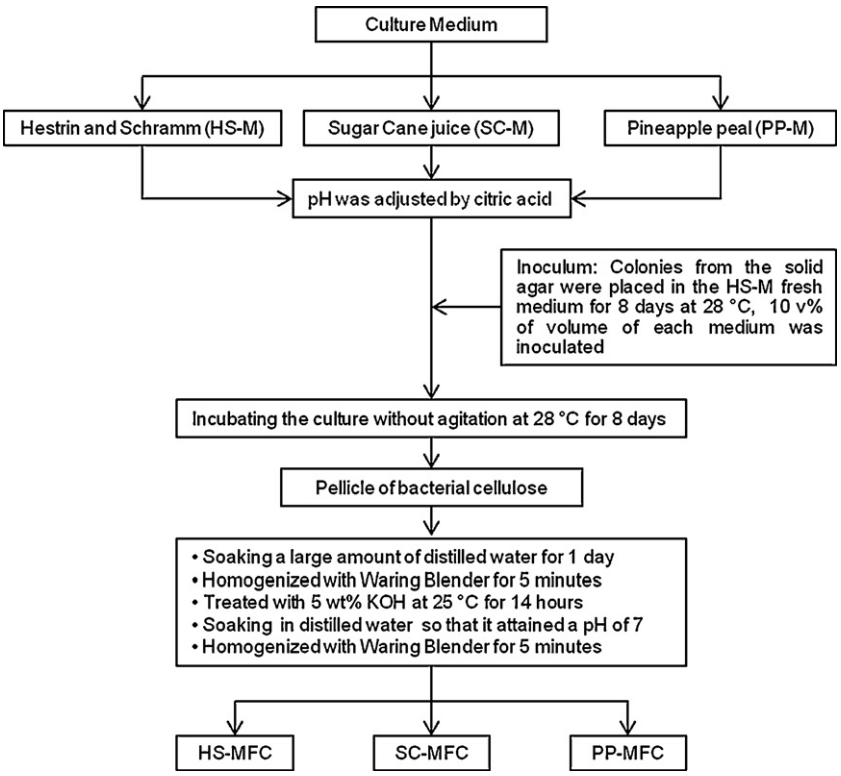

Fig. 1. Scheme for the production of bacterial cellulose from different culture media.

large-scale industrial production, the use of bacterial cellulose is limited (Vandamme, De Baets, Vanbaelen, Joris, & De Wulf, 1998).

In recent years, in order to decrease the costs of bacterial cellulose production, there has been a growing concern to develop culture media based on other sources of sugars like fruits and vegetables (Keshk, Razek, & Sameshima, 2006; Kongruang, 2008; Kurosumi, Sasaki, Yamashita, & Nakamura, 2009; Moon, Park, Chun, & Kim, 2006). In Colombia, there are a lot of organic wastes from different stages of agroindustrial productions that, in many cases, cannot be marketed due to their poor quality. However, they are rich in sugars such as glucose, fructose and sucrose, as well as nitrogen and vitamins that are useful for cellulose biosynthesis.

This work aimed at studying the morphology and structure of bacterial cellulose produced from Colombian agroindustrial residues like pineapple peel and sugar cane juice (*i.e.*, no refined sugar sources) as carbon sources. Bacterial cellulose produced into Hestrin and Schramm's medium (Hestrin & Schramm, 1954) was used for comparison. The cellulose microfibrils synthesized in different media were characterized by transmission electron microscopy (TEM), X-ray diffraction (XRD), attenuated total reflection Fourier transform infrared spectroscopy (ATR-FT-IR) and CP/MAS ^{13}C nuclear magnetic resonance (NMR).

2. Materials and methods

2.1. Materials

The *Gluconacetobacter* strain was first isolated from homemade vinegar culture and identified by 16S rRNA method (Arahal, Sánchez, Marcián, & Garay, 2008) as *Gluconacetobacter swingsii sp.* (Dellaglio et al., 2005)

Culture media used for bacterial cellulose production were sugar cane juice (0.008%, w/v, glucose, 0.066%, w/v, fructose, 8.57%, w/v, sucrose, 0.23%, w/v, total nitrogen), pineapple peel juice (2.14%, w/v, glucose, 2.4%, w/v, fructose, 2.10%, w/v, sucrose, 0.31%, w/v, total nitrogen) and Hestrin–Schramm (2%, w/v, glucose, 0.5%, w/v, peptone, 0.5%, w/v, yeast extract, 0.27%, w/v, Na_2HPO_4). Peptone and yeast extract are important in the HS medium as nitrogen source, the quantification of total nitrogen in sugar cane and pineapple peel juice showed that it was not necessary to add any source of nitrogen. The different culture media were filtered before being used to avoid the presence of fibers, acidified to pH 3.5 by the addition of citric acid and autoclaved at 121 °C. The cellulose samples produced from the three media above will be referred to as SC-MFC, PP-MFC and HS-MFC, respectively, in the following.

Experiments were prepared by adding 10 vol.% inoculums to the different media and statically incubating at 28 °C for 13 days. The collected pellicles were washed with water and homogenized in a Waring Blender for 5 min to obtain microfibrils. The microfibrils were treated for 14 h in a 5 wt% KOH solution, rinsed until pH 7, and homogenized in water for 5 min. The treatments and codification of the cellulose obtained from different media are summarized in Fig. 1.

Finally, films of constant thickness (0.1 mm) were prepared from a suspension of different cellulose microfibrils (0.3 wt%) by vacuum filtration and oven-dried at 70 °C for 48 h between glass plates.

2.2. Scanning electron microscopy (SEM)

SEM was used to observe the microorganism morphology and its distribution in the membrane. The membranes were removed from the homemade vinegar medium, dehydrated at room temperature in a graded ethanol series up to 100 vol.% and embedded in paraffin wax. Sections were cut using a rotary microtome until the membrane was seen on the surface. The sample was coated with gold/palladium using an ion sputter coater and observed with a Jeol JSM 5910 LV microscope operated at 20 kV.

2.3. Transmission electron microscopy (TEM)

The samples obtained after chemical and mechanical treatments were diluted in distilled water and sonicated to achieve a good dispersion. Drops of each suspension were deposited onto glow-discharged carbon-coated electron microscopy grids and negatively stained with 2 wt% uranyl acetate. All samples were observed using a Philips CM200 microscope operating at an acceleration voltage of 80 kV. The images were recorded on Kodak SO163 films.

2.4. X-ray diffraction (XRD)

Dry films of cellulose microfibrils were X-rayed using a Panalytical X'Pert Pro MPD equipment operating at the Ni-filtered CuKα_1 radiation wavelength ($\lambda = 0.15406$ nm), generated at a voltage of 45 kV and a filament emission of 40 mA. Data were collected in reflection mode in the 10–30° 2θ-range with a step of 0.013°. The scans preceded at 56.58 s per step.

The d-spacings between the crystal planes were determined using Bragg's law:

$$d = \frac{\lambda}{2 \sin \theta} \quad (1)$$

where θ is the angle between the plane and the diffracted or incident beam and λ is the wavelength of the X-rays. The apparent crystal size (ACS) was calculated using Scherrer's formula:

$$\mathrm{ACS} = \frac{0.9\lambda}{\mathrm{FWHM} \cos \theta} \quad (2)$$

where FWHM is the width of the peak at half the maximum height. θ is Bragg's angle, and λ is the wavelength of the X-rays.

2.5. Attenuated total reflection Fourier transform infrared spectroscopy (ATR-FT-IR)

Before the measurement, the films of cellulose microfibrils were dried for 2 h at 100 °C to remove moisture. FT-IR spectra were recorded on a Nicolet 6700 spectrophotometer in the 4000–400 cm^{-1} range ATR with a diamond crystal. The spectra were recorded with a resolution of 4 cm^{-1} and an accumulation of 256 scans.

2.6. CP/MAS ^{13}C nuclear magnetic resonance (NMR)

Solid-state ^{13}C NMR spectra of the films of cellulose microfibrils were recorded on a Bruker AV-400-WB spectrometer with a triple probe channel of 4 mm, with rotors of ZrO and a stopper of Kel-F at room temperature. The speed of rotation was 8 kHz and the pulse sequence employed was crosspolarization (CP-MAS) ^1H ^{13}C, using a spectral width of 35 kHz, a contact time of 3 ms and a relaxation time of 4 s with decoupling ^1H. The number of scans was 2048. The chemical shift was established in relative ppm to tetramethylsilene (TMS) as primary reference and the signal of adamantine CH_2 (29.5 ppm) was used as secondary reference. In all spectra, the deconvolution in the C1 region was performed by assigning Lorentzian line shape, whereas in the C4 region, Lorentzian and Gaussian functions were used. The mass fraction of I_α was calculated according to the method of Yamamoto and Horii (1993).

3. Results and discussion

The surface pellicle formed by *G. swingsii sp*. from homemade vinegar was examined by SEM. The micrograph in Fig. 2 reveals the rod-shape of the gram-negative cells. Bundles of cellulose microfibrils were observed directly arising from the cell surface

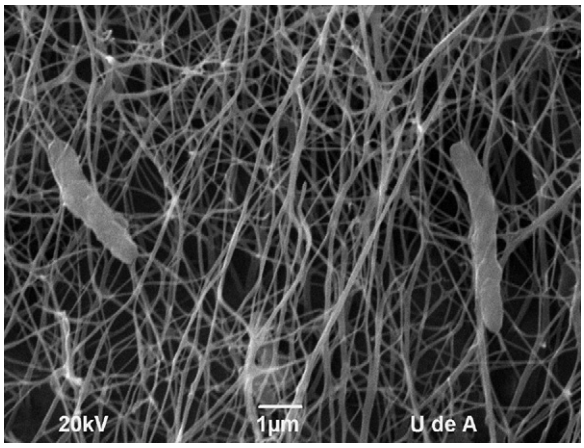

Fig. 2. SEM image of a homemade vinegar pellicle and bacteria with attached cellulose ribbons.

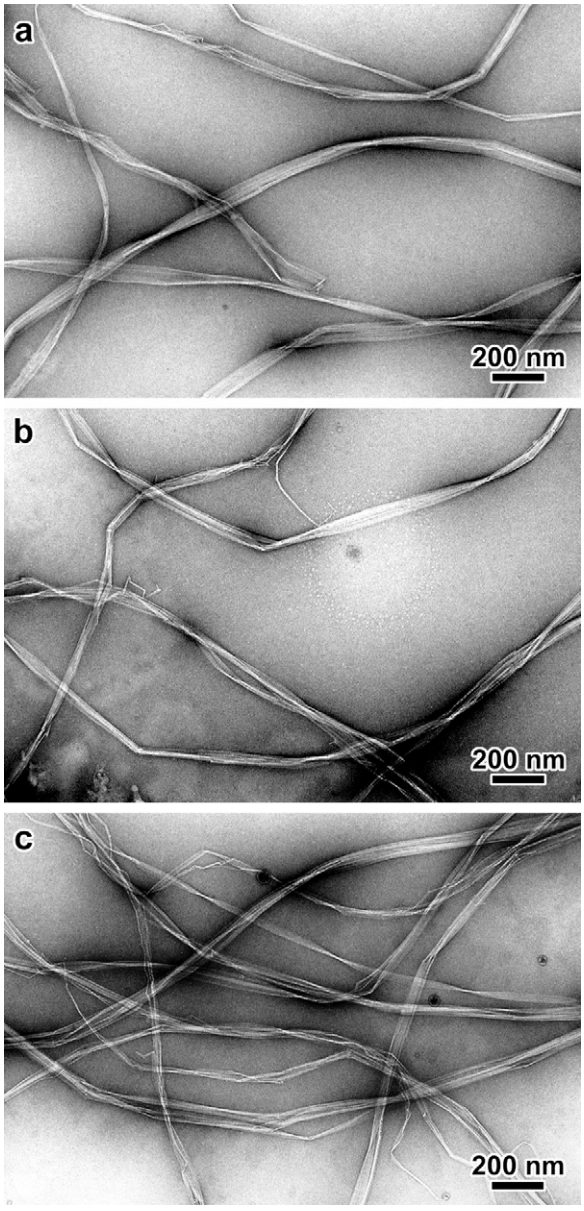

Fig. 3. TEM micrographs of negatively stained preparations of biosynthesized bacterial cellulose ribbons: (a) HS-MFC, (b) SC-MFC, and (c) PP-MFC.

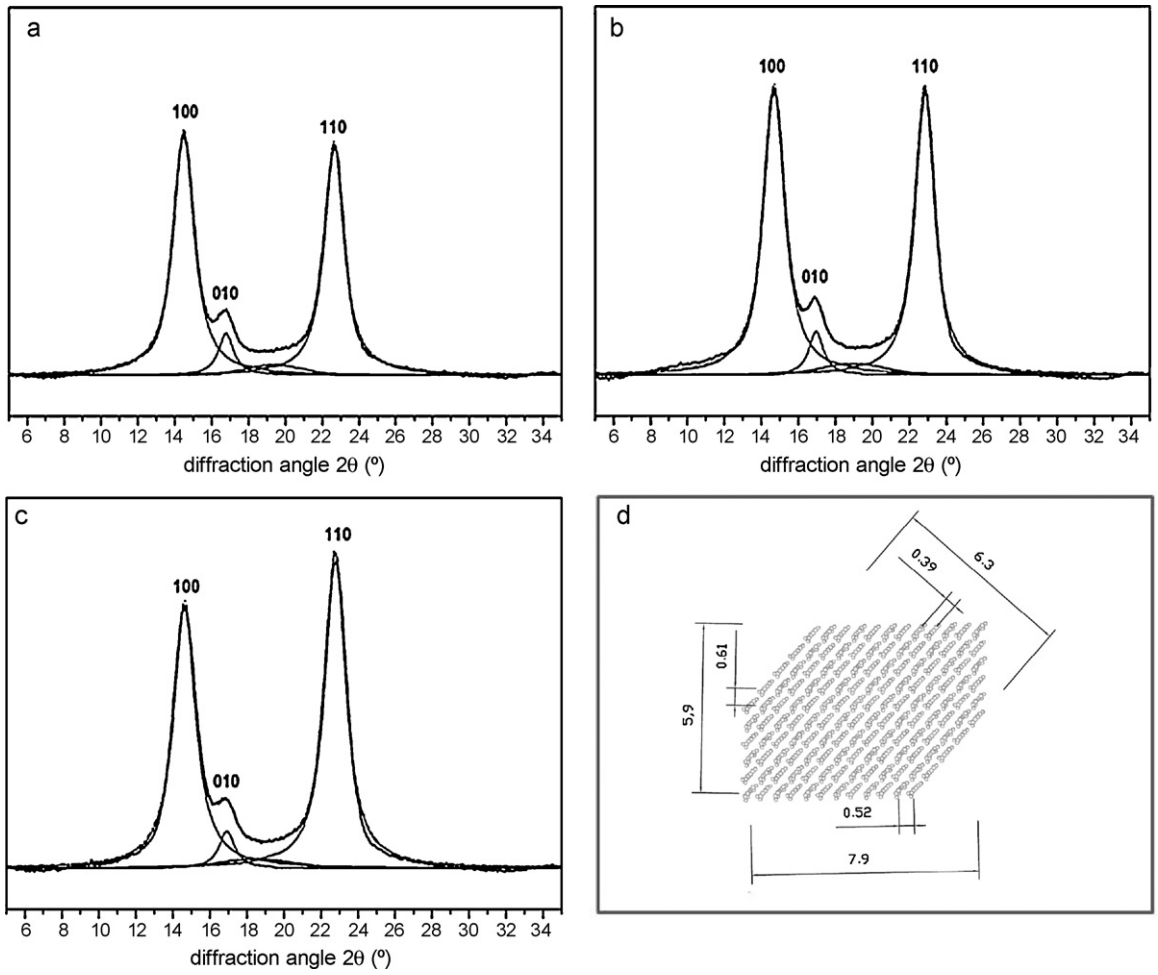

Fig. 4. X-ray diffraction spectra (reflection mode) of films of bacterial cellulose microfibrils produced in different culture media: (a) HS-MFC, (b) SC-MFC, (c) PP-MFC. The indexation is that defined in Sugiyama, Vuong, and Chanzy (1991), (d) suggested cross-section of the bacterial cellulose crystallites. The dimensions, given in nm, were calculated from the width of the X-ray diffraction peaks using Scherrer's equation (Table 1).

and forming a three-dimensional interconnected reticular pellicle at the air–liquid interface (Brown, Willison, & Richardson, 1976).

TEM images recorded from negatively stained specimens are shown in Fig. 3, showing typical 20–70 nm-wide ribbons. Due to the twist of the ribbons, a thickness of 6–8 nm was estimated when the ribbons were seen edge on. Therefore, the ribbons are formed of 3–11 cellulose microfibrils (Brown et al., 1976; Yamanaka & Sugiyama, 2000). The subfibrillation and twisting in all samples likely occurs during mechanical homogenization.

Fig. 4a–c shows that the XRD profiles recorded from the samples are similar to those of the native cellulose produced by Wada, Okano, and Sugiyama (1997). The diffraction patterns were indexed according to the cellulose I_α indexation described by Sugiyama, Persson, and Chanzy (1991). The three visible peaks were assigned to (1 0 0), (0 1 0) and (1 1 0) crystallographic planes, corresponding to diffraction angles of 14.4°, 16.7° and 22.7°, respectively. The contribution of the $(\bar{1}\,1\,2)$ planes was absent in all diffraction patterns. This strong uniplanarity is due to the fact that the cellulose ribbons preferentially oriented parallel to the film surface during drying (Elazzouzi-Hafraoui et al., 2008). The variation in relative peak intensity between the profiles may also be related to small differences in orientation of chains in the three samples. The peaks were deconvoluted using Lorenzian peak functions. Calculated interplanar crystal distances (*d*-spacings) and crystallite dimensions are listed in Table 1. The d_{100}, d_{010} and d_{110} spacings of the SC-MFC and PP-MFC samples are slightly lower than those of the HS-MFC sample. In addition, the PP-MFC crystallite dimensions are smaller than those of SC-MFC and HS-MFC. However, the number of cellulose chains involved appears to be about the same in the three specimens. Atalla and Vanderhart (1984) proposed that native celluloses were composites of I_α and I_β allomorphs. Wada et al. (Wada, Sugiyama, & Okano, 1995; Wada, Okano, & Sugiyama, 2001) proposed that native cellulose I could be classified into a I_α-rich group (algae-bacteria) and a I_β-rich group (cotton-ramie) depending on the characteristic set of *d*-spacings. Wada et al. (1997) observed that the d_{100} and d_{110} spacings of algal-bacterial type were larger than those of cotton-ramie type while d_{010} was smaller (Wada et al., 1997; Wada, Sugiyama, & Okano, 1993). Therefore, the decrease in d_{100} and d_{110} in the case of PP-MFC compared to HS-MFC may be due to a lower amount of I_α allomorph. Differences in *d*-spacings are associated with differences in the cross-sectional dimensions of cellulose crystallites (Bootten et al., 2008; Ioelovich & Larina,

Table 1
d-spacings (*d*) and crystallite size (ACS) in cellulose ribbons synthesized in different media. The indexation is that defined in Sugiyama, Vuong, et al. (1991).

Sample	(1 0 0)		(0 1 0)		(1 1 0)	
	d (nm)	ACS (nm)	*d* (nm)	ACS (nm)	*d* (nm)	ACS (nm)
HS-MFC	0.61	5.9	0.53	7.9	0.39	6.3
SC-MFC	0.60	6.0	0.52	8.4	0.39	6.5
PP-MFC	0.60	5.6	0.52	7.8	0.39	6.0
HS-REF[a]	0.61	7.1	0.53	10.7	0.39	8.1

[a] Determined by X-ray diffractometry by Tokoh et al. (2002b).

1999). The data in Table 1 were used to propose a cross-sectional geometry of the microfibrils synthesized by the microorganism. The results are shown in Fig. 4d. In these arrangements, the elementary crystallites are also ribbon-like with a cross-section of about 8 nm × 6 nm and contain between 150 and 180 chains, in agreement with the TEM images and previous results (Tokoh et al., 1998). PP-MFC presented a smaller crystal size with a smaller number of chains compared with HS-MFC. The difference in these parameters may be associated with substances in the culture medium that can affect the assembling of chains within the crystallite (Tokoh et al., 2002a). Such substances may be present in agro-industrial waste, the pineapple peel containing several carbohydrates such as glucose, fructose, sucrose, rhamanose, galactose, arabinose, xylose, mannose, among others (Larrauri, Rúperez, & Calixto, 1997; Smith & Harris, 1995). Among these carbohydrates, xylose (12–23%) and galactose (10–30%) are present in a high proportion.

The FT-IR spectra of cellulose samples prepared from the different media are shown in Fig. 5a. PP-MFC, SC-MFC and HS-MFC spectra are similar, indicating that cellulose has the same chemical structure. These bands are typical of IR spectra recorded from cellulose of bacterial origin (Hirai et al., 1998; Shirk & Greathouse, 1952; Yamamoto & Horii, 1996). Besides, the spectra showed the characteristic bands of cellulose I, with strong bands at 1429 and 1111 cm^{-1} assigned to CH_2 symmetrical bending and C–O bond stretching, respectively, and a weak and broad band centered at about 897 cm^{-1}, typical of β-linked glucose polymers. Other bands at 1375 cm^{-1} (C–H bending), 1335 cm^{-1} (O–H in-plane bending), 1315 cm^{-1} (CH_2 wagging), 1277 cm^{-1} (C–H bending) and 1225 cm^{-1} (O–H in-plane) indicated the presence of crystalline regions within the structure (Nelson & O'Connor, 1964).

Fig. 5b and c shows the enlargement of the 3720–2650 cm^{-1} and 780–400 cm^{-1} regions of ATR-FTIR spectra, respectively. The absorbances at 3240 and 750 cm^{-1} were assigned to the triclinic I_α allomorph, and the absorbances at 3270 and 710 cm^{-1} were assigned to the monoclinic I_β form (Kataoka & Kondo, 1996; Sugiyama, Persson, et al., 1991). Therefore, the synthesized cellulose contained both allomorphs. This agrees with what was found for native cellulose (Atalla & Vanderhart, 1984). Furthermore, the presence of a prominent band at 3240 cm^{-1} allowed classifying the samples in the *Valonia* and bacterial cellulose family (Marrinan & Man, 1956).

The fraction of each constituting allomorph was determined by CP/MAS ^{13}C NMR. The corresponding spectra are shown in Fig. 6a. They are very similar for all samples, presenting resonance lines assigned to the C1 (102–108 ppm), C4 (81–93 ppm) and C6 (60–70 ppm) carbons, as well as a cluster of resonances assigned to the C2, C3 and C5 carbons (Atalla & VanderHart, 1999; VanderHart & Atalla, 1984). Singlets at C1 and C6 and a doublet at C4 allow the sample classification in the family of *Valonia-Acetobacter*. As expected, in the three cases, the main crystalline form is I_α but the C1 resonance line, also composed of a small doublet beside of central line, may be due to the presence of a minor fraction of I_β (Atalla & Vanderhart, 1984). Further analysis of the spectra can be made to quantify the amount of each allomorph in the samples. The contribution of each allomorph was determined by deconvoluting the C1 and C4 triplets into several constituting lines, on the basis of the model proposed by Atalla and Vanderhart (1984). Each line was assumed to be a Lorentzian function as reported by Yamamoto and Horii (1993). Fig. 6b and c shows the results obtained for C1 and C4 resonances of each sample after deconvolution, respectively. A combination of the I_α and I_β spectra is seen. The C1 resonance is composed of three peaks corresponding to both allomorphs. The main contribution is located at 106.2 ppm, indicating that the samples are I_α-rich. The two side-peaks revealed the presence of a lesser amount of I_β. Moreover, in the case of PP-MFC, the contribution of I_α decreased while that of the I_β side-peaks increased. In this same

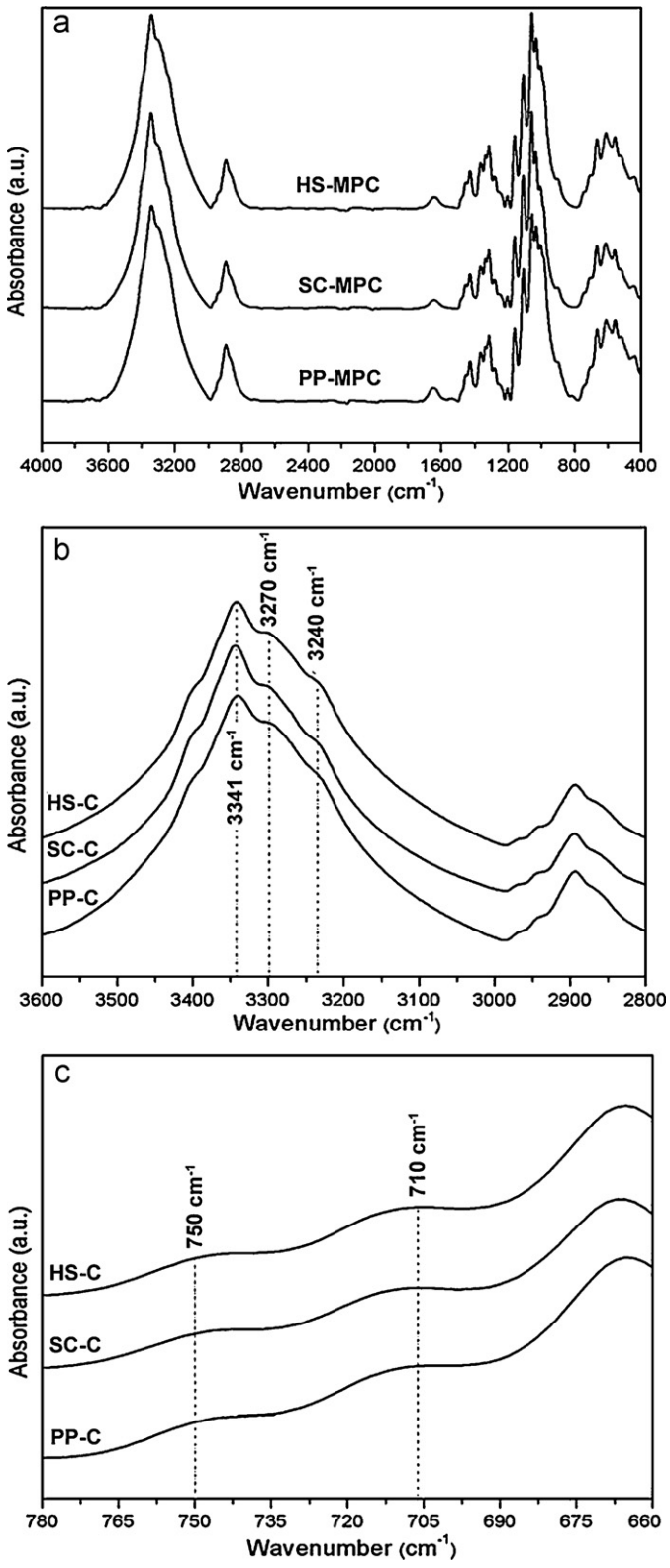

Fig. 5. ATR-FTIR spectra of cellulose microfibrils produced from different culture media: (a) Hestrin & Schramm (HS-MFC), sugar cane juice (SC-MFC), pineapple peel (PP-MFC); (b) absorption bands at 3240 and 3271 cm^{-1} correspond to I_α and I_β, respectively; (c) absorption bands at 750 and 710 cm^{-1} correspond to I_α and I_β, respectively.

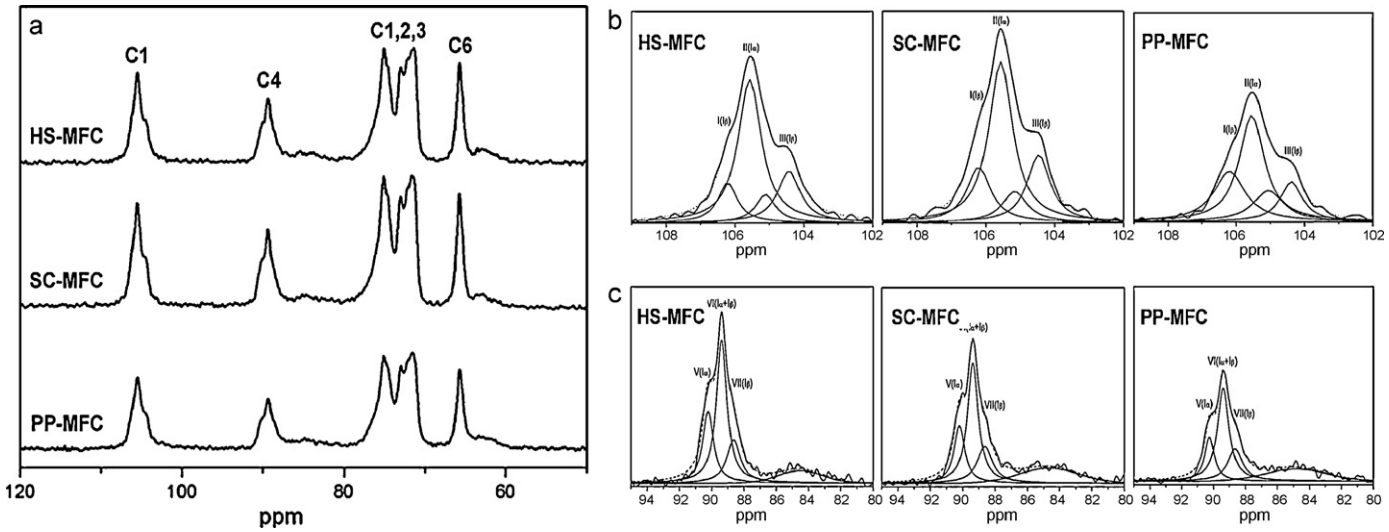

Fig. 6. ^{13}C CP/MAS NMR spectra of cellulose microfibrils produced from different media: (a) HS-MFC, SC-MFC, PP-MFC. The indexation is that defined in VanderHart and Atalla (1984); (b) fit C1 region of the spectra of cellulose microfibrils produced from different media, (c) fit C4 region of the spectra of cellulose microfibrils produced from different media.

Table 2
Fractions of the lines of C1 and C4 triplets for the cellulose microfibrils produced in different media, calculated after a fit of the CP/MAS ^{13}C spectra.

Sample	C1				C4				
	f_I	f_{II}	f_{III}	f_α [a]	f_V	f_{VI}	f_{VII}	f_α [b]	X
HS-MFC	0.133	0.570	0.201	0.602	0.290	0.530	0.203	0.587	0.762
SC-MFC	0.177	0.512	0.207	0.547	0.247	0.528	0.226	0.521	0.767
PP-MFC	0.262	0.438	0.144	0.490	0.216	0.547	0.237	0.479	0.723
HS-REF	–	–	–	–	–	–	–	0.638[c]	0.710[d]

[a] $f_\alpha = (1 - f_I + 2f_{II} - f_{III})/3$.
[b] $f_\alpha = 0.5 + f_V - f_{VII}$.
[c] Determined by CP/MAS ^{13}C NMR (Yamamoto & Horii, 1994).
[d] Determined by CP/MAS ^{13}C NMR (Watanabe et al., 1998).

way, the C4 resonance reveals the contribution of three peaks at 90, 89, 88 ppm for I_α, $I_{(\alpha+\beta)}$ and I_β, respectively. The behavior described for the C1 resonance is also observed for the C4 resonance, revealing a higher amount of I_β allomorph. The mass fraction of both allomorphs in the samples was determined using the method by Yamamoto and Horii (1993) and the results are showed in Table 2. The I_α fraction determined from the C1 and C4 resonances in good agreement. In this case, the cellulose from PP-M contains a smaller amount of I_α than HS-M and SC-M. A similar result was mentioned in other works reporting on the crystallinity changes in bacterial cellulose produced in HS medium in the presence of other cell wall polysaccharides like mannan and xylan (Tokoh et al., 1998; Tokoh et al., 2002b; Whitney et al., 1998; Yamamoto & Horii, 1994).

Moreover, the abundance of crystallites relative to amorphous cellulose was determined according to Newman (1999) and is presented in Table 2. The crystallinity of SC-MFC remains invariant, but a decrease is observed for PP-MFC when compared with HS-MFC. This may be due to the specific composition of the culture medium inducing differences in the crystallization process of cellulose (Yamamoto & Horii, 1994). Apparently, the aggregation of cellulose chains into a normal ribbon is hindered by the other polysaccharides that can adhere to the surface of the subfibrils extruded by the microorganism (Yamamoto & Horii, 1996). This is shown by the decrease in crystal size observed for PP-MFC.

4. Conclusions

The morphological, chemical and structural characteristics of cellulose produced in non-conventional culture media from Colombian agroindustrial wastes like pineapple peel and sugar cane juice were examined. SEM images show a three-dimensional pellicle interconnected in a reticular structure and the TEM images show typical 20–70 nm-wide ribbons. While in the ATR-FT-IR spectra, it was observed that the chemical structure of the microfibrils was unaffected by the different conditions, crystalline parameters determined from XRD and ^{13}C NMR profiles suggest that these were slightly affected in the case of cellulose produced in pineapple peel medium. This may be due to the presence of other polysaccharides driving changes in the aggregation of cellulose chains into the microfibrils. ATR-FT-IR, XRD and ^{13}C NMR indicate that the triclinic I_α and monoclinic I_β crystalline forms are presented, but the I_α allomorph is in a slightly smaller amount in the sample prepared in pineapple peel medium.

The production of bacterial cellulose was relatively high with similar properties to that produced in Hestrin and Schramm's medium. These results suggest that it is possible to produce bacterial cellulose from low-cost resources in order to increase its production to a larger scale.

Acknowledgments

The authors would like to thank Colciencias and SENA for financial support as well as Y. Nishiyama (CERMAV) for helpful suggestions.

References

Arahal, D. R., Sánchez, E., Marcián, M. C., & Garay, E. (2008). Value of *recN* sequences for species identification and as a phylogenetic marker within the family "*Leuconostocaceae*". *International Microbiology: The Official Journal of the Spanish Society for Microbiology*, *11*(1), 33–39.

Atalla, R. H., & Vanderhart, D. L. (1984). Native cellulose: A composite of two distinct crystalline forms. *Science*, *223*(4633), 283–285.

Atalla, R. H., & VanderHart, D. L. (1999). The role of solid state ^{13}C NMR spectroscopy in studies of the nature of native celluloses. *Solid State Nuclear Magnetic Resonance*, *15*(1), 1–19.

Bielecki, S., Krystynowicz, A., Turkiewicz, M., & Kalinowska, H. (2005). Bacterial cellulose. In Alexander Steinbüchel, & Yoshiharu Doi (Eds.), *Biotechnology of polymer: From synthesis to patents* (pp. 381–434). Weinheim, Germany: Wiley-VCH. Chapter 14.

Bootten, T. J., Harris, P. J., Melton, L. D., & Newman, R. H. (2008). WAXS and 13C NMR study of *Glucoacetobacter xylinus* cellulose in composites with tamarind xyloglucan. *Carbohydrate Research*, *343*(2), 221–229.

Brown, A. J. (1886a). On an acetic ferment which forms cellulose. *Journal of the Chemical Society*, *49*, 432–439.

Brown, A. J. (1886b). The chemical action of pure cultivations of bacterium aceti. *Journal of the Chemical Society*, *49*, 172–187.

Brown, R. M., Jr., Willison, J. H. M., & Richardson, C. L. (1976). Cellulose biosynthesis in *Acetobacter xylinum*: Visualization of the site of synthesis and direct measurement of the in vivo process. *Proceedings of the National Academy of Science of the United States of America*, *73*(12), 4565–4569.

Dellaglio, F., Cleenwerck, I., Felis, G. E., Engelbeen, K., Janssens, D., & Marzotto, M. (2005). Description of *Gluconacetobacter Swingsii sp. Nov.* and *Gluconacetobacter rhaeticus sp. nov.*, isolated from Italian apple fruit. *International Journal of Systematic and Evolutionary Microbiology*, *55*(6), 2365–2370.

Elazzouzi-Hafraoui, S., Nishiyama, Y., Putaux, J.-L., Heux, L., Dubreuil, F., & Rochas, C. (2008). The shape and size distribution of crystalline nanoparticles prepared by acid hydrolysis of native cellulose. *Biomacromolecules*, *9*(1), 57–65.

Fontana, J. D., De Souza, A. M., Fontana, C. K., Torriani, I. L., Moresch, J. C., Gallotti, B. J., et al. (1990). Acetobacter cellulose pellicle as a temporary skin substitute. *Applied Biochemistry and Biotechnology*, *24*(25), 253–264.

Heo, M., & Son, H. (2002). Development of an optimized, simple chemically defined medium for bacterial cellulose production by *Acetobacter* sp. A9 in shaking cultures. *Biotechnology and Applied Biochemistry*, *36*(1), 41–45.

Hestrin, S., & Schramm, M. (1954). Synthesis of cellulose by *Acetobacter xylinum*. 2. Preparation of freeze-dried cells capable of polymerizing glucose to cellulose. *Biochemical Journal*, *58*(2), 345–352.

Hirai, A., Tsuji, M., Yamamoto, H., & Horii, F. (1998). In situ crystallization of bacterial cellulose. III. Influences of different polymeric additives on the formation of microfibrils as revealed by transmission electron microscopy. *Cellulose*, *5*(3), 201–213.

Iguchi, M., Yamanaka, S., & Budhiono, A. (2000). Review: Bacterial cellulose—A masterpiece of nature's arts. *Journal of Materials Science*, *35*(2), 261–270.

Ioelovich, M., & Larina, E. (1999). Parameters of crystalline structure and their influence on the reactivity of cellulose I. *Cellulose Chemistry & Technology*, *33*(1–2), 3–12.

Jonas, R., & Farah, L. (1998). Production and application of microbial cellulose. *Polymer Degradation and Stability*, *59*(1–3), 101–106.

Kataoka, Y., & Kondo, T. (1996). Changing cellulose crystalline structure in forming wood cell walls. *Macromolecules*, *29*(19), 6356–6358.

Keshk, S., Razek, T., & Sameshima, K. (2006). Bacterial cellulose production from beet molasses. *African Journal of Biotechnology*, *5*(17), 1519–1523.

Klemm, D., Shumann, D., Udhardt, U., & Marsch, S. (2001). Bacterial synthesized cellulose—Artificial blood vessels for microsurgery. *Progress in Polymer Science*, *26*(9), 1561–1603.

Kongruang, S. (2008). Bacterial cellulose production by *Acetobacter xylinum* strains from agricultural waste products. *Applied Biochemistry and Biotechnology*, *148*(1–3), 245–256.

Kurosumi, A., Sasaki, C., Yamashita, Y., & Nakamura, Y. (2009). Utilization of various fruit juices as carbon source for production of bacterial cellulose by *Acetobacter xylinum* NBRC 13693. *Carbohydrate Polymers*, *76*(2), 333–335.

Larrauri, J. A., Rúperez, P., & Calixto, F. S. (1997). Pineapple shell as a source of dietary fiber with associated polyphenols. *Journal of Agricultural and Food Chemistry*, *45*(10), 4028–4031.

Marrinan, H., & Mann, J. (1956). Infrared spectra of the crystalline modification of cellulose. *Journal of Polymer Science*, *21*(98), 301–311.

Moon, S., Park, J., Chun, H., & Kim, S. (2006). Comparisons of physical properties of bacterial cellulose produced in different culture conditions using saccharified food wastes. *Biotechnology and Bioprocess Engineering*, *11*(1), 26–31.

Nakagaito, A. N., Masaya Nogi, M., & Yano, H. (2010). Displays from transparent films of natural nanofibers. *MRS Bulletin*, *35*(3), 214–218.

Nelson, M., & O'Connor, R. (1964). Relation of certain infrared bands to cellulose crystallinity and crystal lattice type. Part I. Spectra of lattice types I, II, III and of amorphous cellulose. *Journal of Applied Polymer Science*, *8*(3), 1311–1324.

Newman, R. (1999). Estimation of the lateral dimensions of cellulose crystallites using 13C NMR signal strengths. *Solid State Nuclear Magnetic Resonance*, *15*(1), 21–29.

Ramanaka, K., Tomar, A., & Singh, L. (2000). Effect of various carbon and nitrogen sources on cellulose synthesis by *Acetobacter xylinum* in world. *Journal of Microbiology and Biotechnology*, *16*(3), 245–248.

Shirk, H., & Greathouse, G. (1952). Infrared spectra of bacterial cellulose. *Analytical Chemistry*, *24*(11), 1774–1775.

Smith, B. G., & Harris, P. J. (1995). Polysaccharide composition of unlignified cell walls of pineapple [*Ananas comosus* (L.) Merr.] fruit. *Plant Physiology*, *107*(4), 1399–1409.

Sugiyama, J., Persson, J., & Chanzy, H. (1991). Combined infrared and electron diffraction study of the polymorphism of native cellulose. *Macromolecules*, *24*(9), 2461–2466.

Sugiyama, J., Vuong, R., & Chanzy, H. (1991). Electron diffraction study on the two crystalline phases occurring in native cellulose from an algal cell wall. *Macromolecules*, *24*(14), 4168–4175.

Tokoh, C., Takabe, K., Sujiyama, J., & Fujita, M. (2002a). CP/MAS 13C NMR and electron diffraction study of bacterial cellulose structure affected by cell wall polysaccharides. *Cellulose*, *9*(3–4), 351–360.

Tokoh, C., Takabe, K., Sujiyama, J., & Fujita, M. (2002b). Cellulose synthesized by *Acetobacter xylinum* in the presence of plant cell wall polysaccharides. *Cellulose*, *9*(1), 65–74.

Tokoh, C., Takabe, K., Fujita, M., & Saiki, H. (1998). Cellulose synthesized by *Acetobacter xylinum* in presence of acetyl glucomannan. *Cellulose*, *5*(4), 249–261.

Vandamme, E., De Baets, S., Vanbaelen, A., Joris, K., & De Wulf, P. (1998). Improved production of bacterial cellulose and its application potential. *Polymer Degradation and Stability*, *59*(1–3), 93–99.

VanderHart, D., & Atalla, R. (1984). Studies of microstructure in native celluloses using solid-state ^{13}C NMR. *Macromolecules*, *17*(8), 1465–1472.

Wada, M., Sugiyama, J., & Okano, T. (1993). Native cellulose on the basis of two crystalline phase (I/I) system. *Journal of Applied Polymer Science*, *49*(8), 1491–1496.

Wada, M., Sugiyama, J., & Okano, T. (1995). Two crystalline phases (Iα/Iβ) system of native celluloses in relation to plant phylogenesis. *Mokusai Gakkaishi*, *41*(2), 186–192.

Wada, M., Okano, T., & Sugiyama, J. (1997). Synchrotron-radiated X-ray and neutron diffraction study of native cellulose. *Cellulose*, *4*(3), 221–232.

Wada, M., Okano, T., & Sugiyama, J. (2001). Allomorphs of native cellulose I evaluated by two equatorial d-spacing. *Journal of Wood Science*, *47*(2), 124–128.

Watanabe, K., Tabuchi, M., Moringa, Y., & Yoshinaga, F. (1998). Structural features and properties of bacterial cellulose produced in agitated culture. *Cellulose*, *5*(3), 187–200.

Whitney, S., Brigham, J., Darke, A., Reid, J., & Gidley, M. (1998). Structural aspects of the interaction of mannan-based polysaccharides with bacterial cellulose. *Carbohydrate Research*, *307*(3–4), 299–309.

Yamamoto, H., & Horii, F. (1993). CP/MAS 13C NMR analysis of the crystal transformation induced for *Valonia* cellulose by annealing at high temperature. *Macromolecules*, *26*(6), 1313–1317.

Yamamoto, H., & Horii, F. (1994). In situ crystallization of bacterial cellulose I. Influences of polymeric Additives, stirring and temperature on the formation cellulose I_α and I_β as revealed by cross polarization/magic angle spinning (CP/MAS) ^{13}C NMR spectroscopy. *Cellulose*, *1*(1), 57–66.

Yamamoto, H., & Horii, F. (1996). In situ crystallization of bacterial cellulose II. Influences of polymeric Additives, stirring and temperature on the formation cellulose Iα and Iβ at the early stage of incubation. *Cellulose*, *3*(1), 229–242.

Yamanaka, S., & Sugiyama, J. (2000). Structural modification of bacterial cellulose. *Cellulose*, *7*(3), 213–225.